

Wettability read-out strategy for aptamer target binding based on a recognition/hydrophobic bilayer surface

Yunfei Fan,^[a] Yahang Xie,^[a] Zhen Zhao,^[a] Yang Zhao,^[b] Rui Yu,^[a] Xiang-yang Liu,^[a] Youhui Lin,^[a]
Changxu Lin^{[a]*}

[a] Research Institute for Biomimetics and Soft Matter, Fujian Provincial Key Laboratory for Soft Functional Materials Research, College of Physical Science and Technology, Xiamen University, 9 Zengcuoan West Road, 361005 Xiamen, China

[b] Institute of Forensic Science, Ministry of Public Security, 100038, Beijing, China

Experimental Procedures

1 Chemicals and DNA strands

Ethanol and sodium hydroxide were purchased from Xilong Chemical. Cobalt chloride hexahydrate was from Sigma Aldrich. Triethoxy-1H, 1H, 2H, 2H-trifluorooctylsilane and urea was from Aladdin Biochemical Technology. Methamphetamine and ephedrine were legal sample from Institute of Forensic Science, Ministry of Public Security of China. All reagents were analytical degree and used without further purification. Single strand DNA oligomers were synthesized by Sangon Biotech (Shanghai) with the sequence listed below. Ultrapure (Milli-Q) water was from Milli-Q water system (Millipore).

Table S1. Detail of single strand DNA oligomer

Sequence Abbreviation	Sequence
MA	5'-ACG GTT GCA AGT GGG ACT CTG GTA GGC TGG GTT AAT TTG G-3'
MIS_1	5'-TGC CAA CGT TGT GGG ACT CTG GTA GGC TGG GTT AAT TTG G-3'
MIS_2	5'-ACG GTT GCA A CA CCC TGA GAG GTA GGC TGG GTT AAT TTG G-3'

MIS_3	5'-ACG GTT GCA AGT GGG ACT CTC CAT CCG ACC GTT AAT TTG G-3'
MIS_4	5'-ACG GTT GCA AGT GGG ACT CTG GTA GGC TGG CAA TTA AAC C -3'

2 Fabrication of sensor units

Growth of aptamers: After centrifuging the oligo at 4000 r/min for 30 -60 S. Opening the lid of the centrifuge tube slowly, adding appropriate amount of water, covering the lid, shaking well, mixing and storing in a refrigerator at -20°C. Subsequently, the slide was immersed in sodium hydroxide solution for 24 hours, taken out and rinsed with distilled water and dried for use. Finally, the oligomer solution was evenly dropped on a clean glass slide (2.5 cm*0.8 cm) and dried at room temperature.

Growth of nanoneedles: 0.9 g of cobalt chloride hexahydrate and 5 g of urea were weighed and dissolved in 25 mL of deionized water and recorded as solution A. The treated slide and solution A were placed together in a 15 mL centrifuge tube, then the centrifuge tube was placed in a drying oven at 60°C for 24 hours. After the hydrothermal reaction was completed, the brucite-type cobalt hydroxide (BCH, $\text{Co}(\text{OH})_{1.13}\text{Cl}_{0.09}(\text{CO}_3)_{0.39}\cdot 0.05\text{H}_2\text{O}$) nanoneedle surface was fabricated. The slides with BCH nanoneedles were taken out and rinsed with distilled water and dried for later use.

Hydrophobic substance modification: Measuring 100 μL of triethoxy-1H, 1H, 2H, 2H-trifluoro-n-octylsilane, dissolving in 5 mL of ethanol solution, and dilute to 10 mL with deionized water. The needle-like surface obtained in the previous step was immersed in a fluorosilane solution, placed in a centrifuge tube, and allowed to stand at room temperature for 15 minutes. After the end of the standing, the sample is taken out and dried, which is the desired hydrophobic sensor unit.

3 Characterization

Scanning electron microscopy detection: The sample was fixed to the sample stage with a conductive paste and then sprayed with platinum. The observation was completed on Hitachi SU-70.

Contact angle detection: The liquids tested were aqueous solutions, 0.01 mol/L, 0.1

mol/L methamphetamine (MA) solution and 0.1 mol/L ephedrine (EPH) solution in water. The introduction of ephedrine contact angle signal analysis can determine the accuracy of the sensing unit. The test method is static contact angle mode, and the solution is directly dropped on the sensor surface. The droplet size is 10 μ L. The contact angle meter was Dataphysics DSA100. The temperature manipulation was conducted with heating stage Cossim KEL-2000 (<https://www.pelttech.com/>).

Fluorescence microscopy detection: The 3' end of the methamphetamine aptamer was modified with cy3, and the methamphetamine aptamer in the experiment was replaced with the modified fluorescent aptamer. The resulting sensor unit was then observed and photographed on the fluorescence microscope Leica DFC7000T. The excitation wavelength is 550 nm.

Supplementary Results

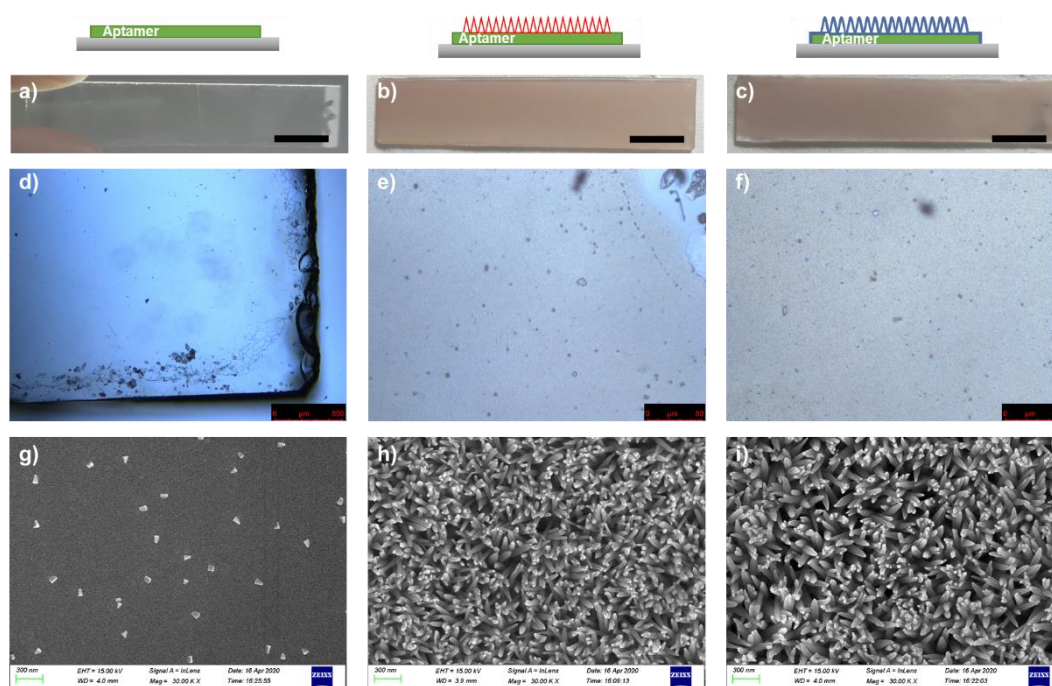


Figure S1. Optical picture (a-c), microscopic picture (d-f), SEM image (g-i) of aptamer-supported hydrophobic surfaces at different fabrication stage by AHS-MA-0.1 as the example: a) after aptamer coating, b) after growth of BCH nanoneedles, c) after hydrophobic coating of fluorosilane. Scale bar in (a-c): 1 cm.

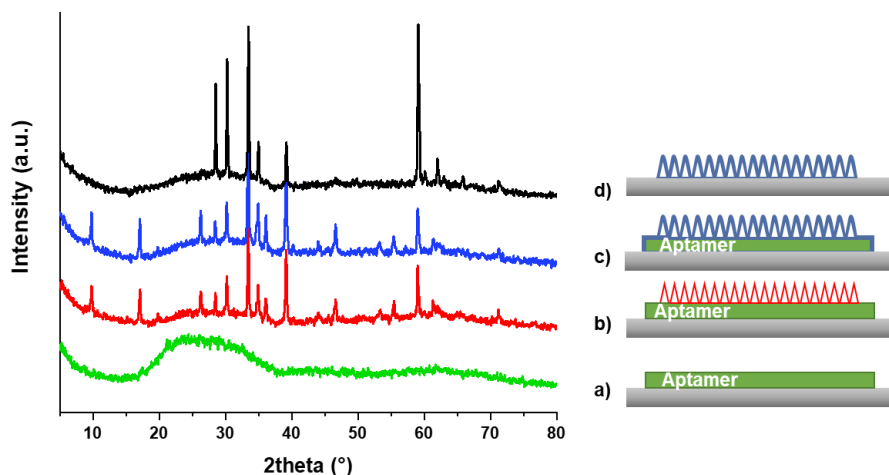


Figure S2. XRD pattern of aptamer-supported hydrophobic surfaces at different fabrication stage by AHS-MA-0.1 as the example: a) after aptamer coating, b) after growth of BCH nanoneedles, c) after hydrophobic coating of fluorosilane. d) fluorosilane-treated hydrophobic nanoneedles coating directly on the substrate without aptamer layer as the control.

Remark: the XRD pattern of BCH nanoneedle was consistent with the original report (E. Hosono, S. Fujihara, I. Honma and H. Zhou, *Journal of the American Chemical Society*, 2005, **127**, 13458-13459.)

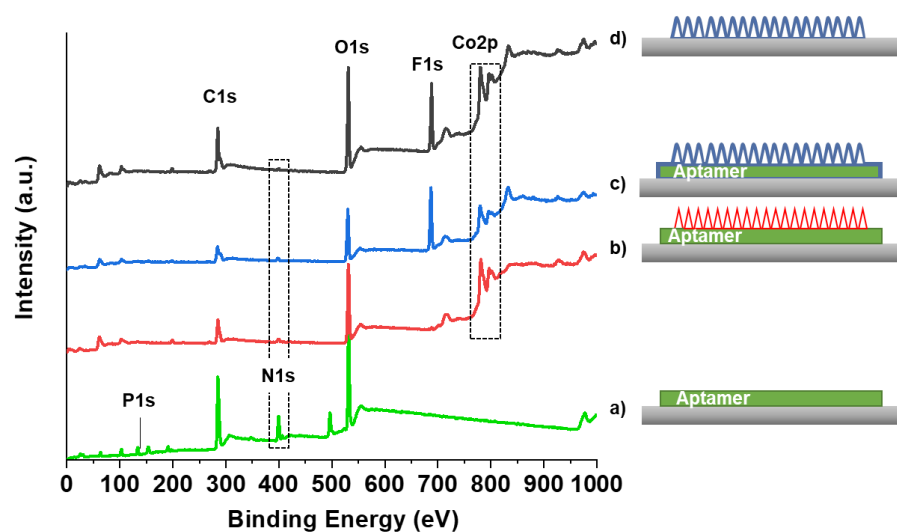


Figure S3. XPS survey spectrum of aptamer-supported hydrophobic surfaces at different fabrication stage by AHS-MA-0.1 as the example: a) after aptamer coating, b) after growth of BCH nanoneedles, c) after hydrophobic coating of fluorosilane. d) fluorosilane-treated hydrophobic nanoneedles coating directly on the substrate without aptamer layer as the control.

Remark: the XPS result was consistent with the composition variation during the fabrication of AHS. The deposition of aptamers resulted in the introduction of N and P peaks. The growth of BCH nanoneedles was reflected on the introduction of Co2p peaks. Only after the coating of fluorosilane, a F1s peak could be identified.

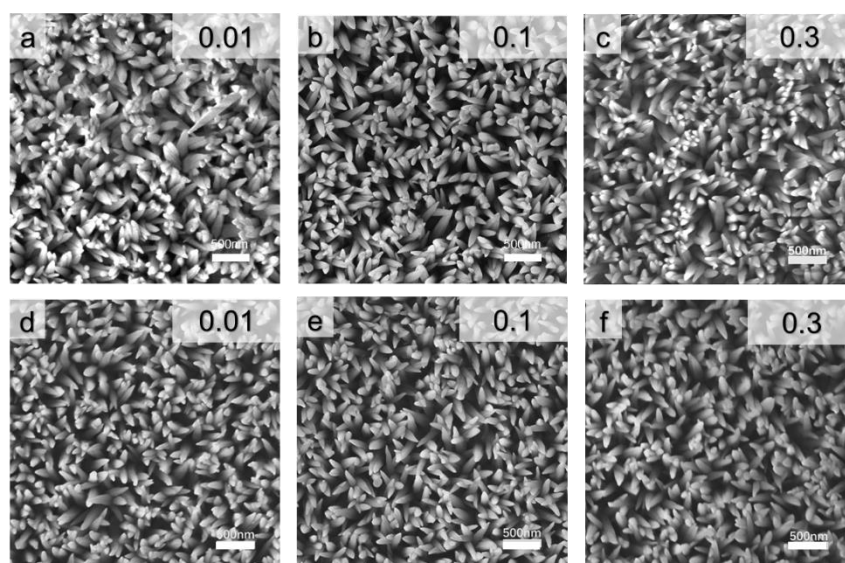


Figure S4. SEM picture of nanoneedle surface: a-c) AHS-MA-0.01, AHS-MA-0.1, AHS-MA-0.3 and d-f) corresponding surface morphology after contact of pure water droplets.

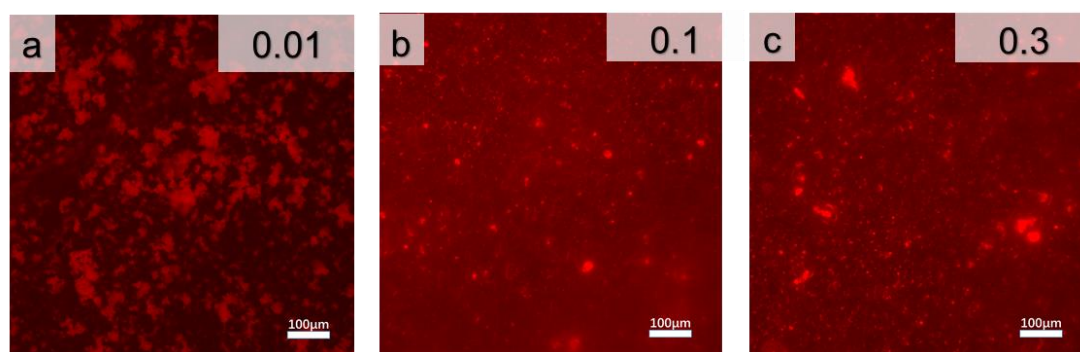


Figure S5. Fluorescent image of cy3 labelled AHS-MA-x. a) AHS-MA-0.01, b) AHS-MA-0.1, c) AHS-MA-0.3.

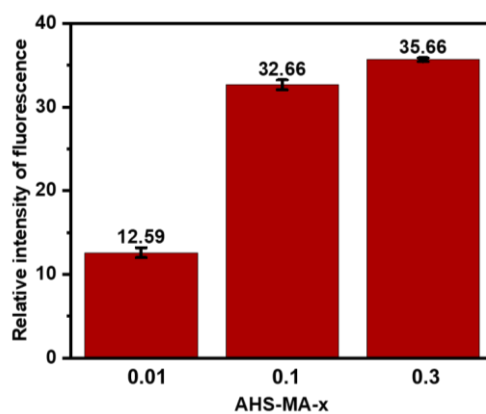


Figure S6. Fluorescence intensity histogram of cy3 labelled AHS-MA-x.

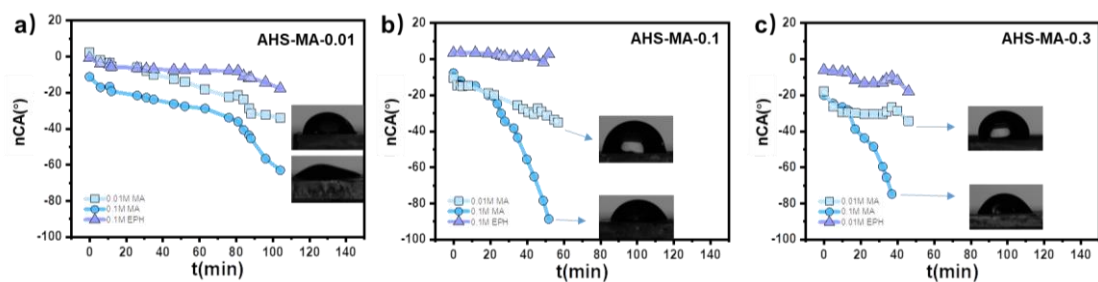


Figure S7. nCA vs. time data of AHS-MA-x at 25°C. In the view of target solution variation.

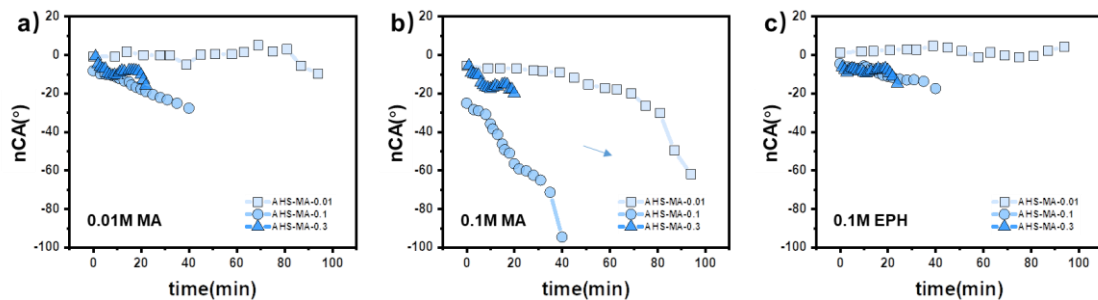


Figure S8. nCA vs. time data of AHS-MA-x at 30°C. In the view of AHS-MA-x variation.

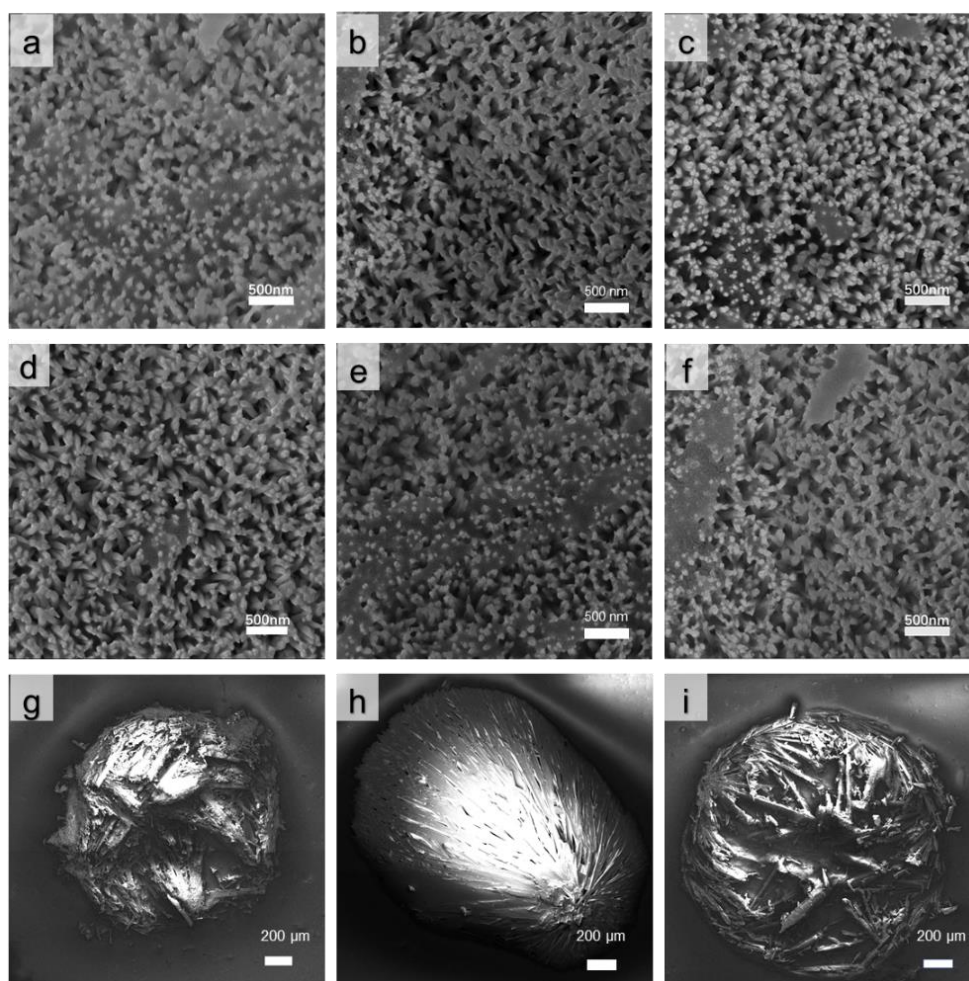
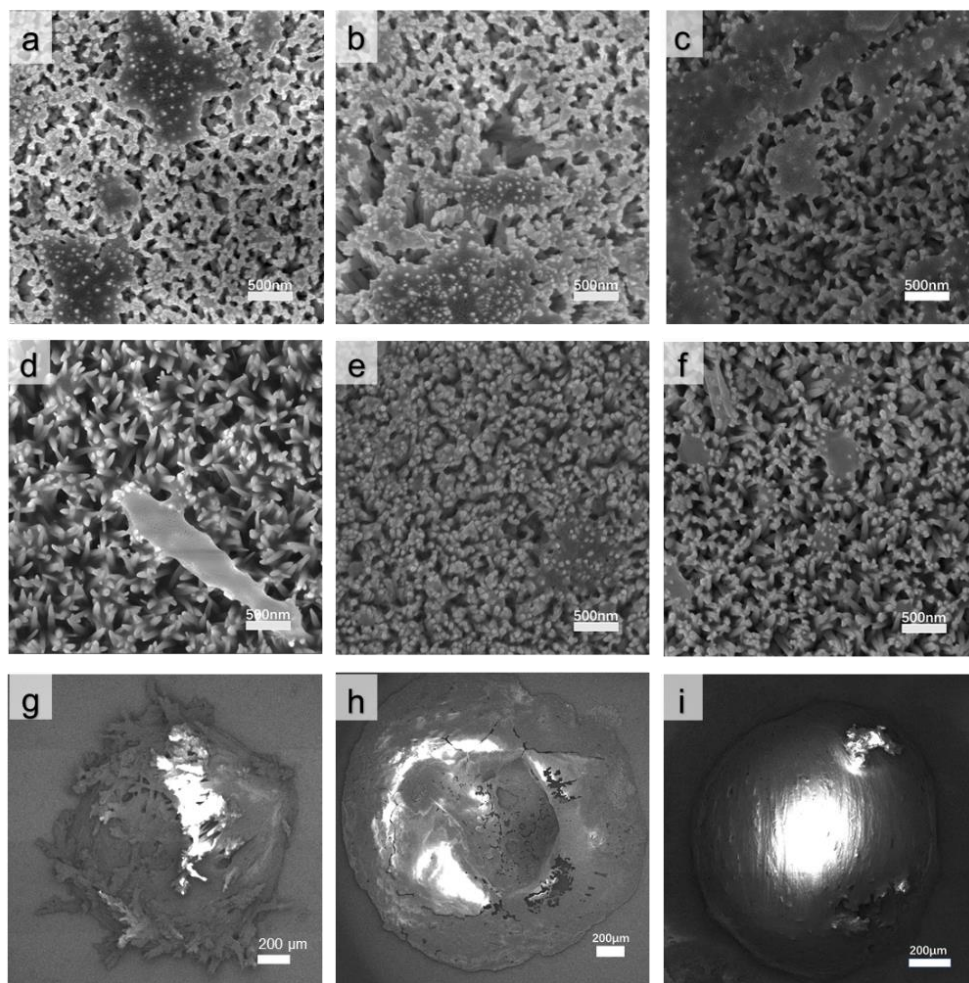


Figure S9. SEM pictures of analyte solution vs. AHS-MA-x orthogonally at 25°C. The combination of each sub-image is at Table S2.

Table S2. Legend of Figure S9 and Figure S10.

AHS-MA-x	0.01	0.1	0.3
0.1M MA	a	b	c
0.01M MA	d	e	f
0.1M EPH	g	h	i

**Figure S10.** SEM pictures of analyte solution vs. AHS-MA-x orthogonally at 30 °C. The combination of each sub-image is at Table S2.

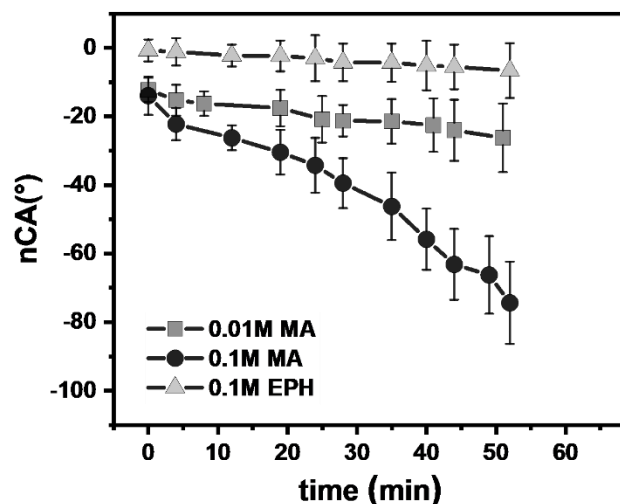


Figure S11. Graph of the net contact angle (nCA) vs time for AHS-MA-0.1 after 14 days since the surface was made

Table S3. CA raw data (degree) of analyte solution vs. time on AHS-MA-x at 25°C. (Fig.2, Fig.S7)

a) $x=0.01$

Time(min)	Blank	0.1M MA	0.01M MA	0.1M EPH
0	126.2	114.9	128.4	125.4
6	126.1	109.0	123.9	122.1
11	125.7	109.0	122.2	121.3
12	125.5	106.2	120.0	119.7
26	124.3	102.7	118.2	117.8
31	123.8	101.0	115.9	116.8
35	123.3	99.5	113.3	116.2
46	120.8	94.5	108.3	113.3
52	119.3	91.6	105.3	111.7
63	115.3	86.4	97.1	107.3
76	109.3	75.4	87.0	101.3
81	105.8	69.6	84.2	97.7
84	103.7	63.0	79.9	92.8
87	101.6	57.9	72.8	89.6
88	101.0	55.5	69.5	89.1
96	95.5	38.9	63.1	81.1
104	87.1	24.0	53.0	69.3

b) $x=0.1$

Time(min)	Blank	0.1M MA	0.01M MA	0.1M EPH
0	139.7±0.2	131.8±3.7	129.1±3.7	143.0±4.2
4	139.6±0.1	127.3±4.3	124.7±2.4	143.0±3.6
8	139.4±0.3	126.0±4.3	124.5±2.8	142.6±3.9
12	139.3±0.3	124.2±4.9	121.7±3.5	139.3±0.3
19	139.0±0.2	118.7±3.7	119.8±3.8	142.0±3.7

Supplementary Information

25	139.6±0.5	114.6±6.1	118.5±5.1	142.0±3.8
28	138.3±0.4	103.6±7.1	116.0±4.6	139.6±3.2
35	136.4±0.5	92.7±8.0	110.5±6.2	137.0±4.4
41	135.1±0.4	79.2±6.3	105.4±7.2	136.8±3.6
44	132.2±0.7	66.7±9.9	101.5±7.6	133.6±4.1
49	128.3±0.4	49.5±8.7	–	–
51	123.6±0.5	–	92.0±5.7	126.2±4.5
52	120.2±0.6	31.2±10.9	–	–

c) $x=0.3$

Time(min)	Blank	0.1M MA	0.01M MA	0.1M EPH
0	146.9	126.8	129.0	140.7
5	144.9	120.2	118.6	138.0
10	142.9	116.3	113.3	135.8
13	140.6	112.3	111.0	133.0
17	139.3	100.5	109.3	127.5
22	137.6	93.7	106.9	124.0
27	128.0	79.4	97.5	114.5
32	118.3	58.6	87.6	105.3
34	115.8	50.2	86.8	104.6
37	110.0	35.2	83.2	100.1
40	107.6	–	78.7	95.5
46	100.7	–	66.3	82.7

Table S4. Raw data of CA on AHS-MA-x at 30°C. (Fig.S8)a) $x=0.01$

Time(min)	Blank	0.1M MA	0.01M MA	0.1M EPH
0	136.1	130.3	135.3	137.2
9	135.7	128.8	134.8	137.5
14	134.5	127.6	136.1	136.5
21	132.7	125.5	132.6	135.2
28	130.6	122.6	130.4	133.5
32	130.2	121.7	129.9	132.9
39	127.8	118.7	122.6	132.5
45	126.0	114.0	126.2	129.9
51	123.4	108.0	123.8	125.5
58	120.3	103.0	120.6	118.9
63	113.4	95.4	114.9	114.7
69	112.7	92.7	117.7	112.3
75	108.4	81.9	110.2	107.1
81	100.3	70.0	103.2	99.8
87	93.2	43.5	87.5	95.3
94	89.3	27.3	79.4	93.6

b) $x=0.1$

Time(min)	Blank	0.1M MA	0.01M MA	0.1M EPH
0	143.8	118.8	135.5	139.2
3	143.7	115.3	133.8	137.5
5	143.5	114.5	133.4	136.9
8	143.5	112.6	132.7	136.5
10	143.3	107.5	131.6	137.6
11	143.2	104.7	130.9	137.0
13	143.1	101.8	129.6	135.9
15	143.0	96.7	128.9	134.8
16	142.8	93.5	127.1	133.5
18	142.8	91.7	126.0	132.2
20	142.6	86.0	124.8	131.4
22	142.5	83.3	123.4	130.8
25	142.3	82.1	121.7	129.7
28	142.0	79.5	119.8	128.9
31	141.8	76.7	118.5	128.9
35	141.6	70.2	116.5	127.9
40	140.4	45.8	112.7	122.9

c) $x=0.3$

Time(min)	Blank	0.1M MA	0.01M MA	0.1M EPH
0	123.97	118.3	123.1	117.5
1	120.83	111.6	116.1	113.1
2	120.13	110.1	113.8	111.0
3	117.81	107.5	110.6	109.8
4	117.3	106.8	110.1	110.2
5	116.6	102.2	107.1	109.2
6	115.54	99.7	105.1	107.6
7	112.47	95.7	101.6	103.8
8	111.4	94.3	101.0	103.4
9	110.83	93.2	100.2	101.7
10	108.6	91.6	99.4	98.9
11	106.93	91.0	98.7	97.9
12	105.31	88.8	96.7	96.9
14	102.66	87.3	94.7	94.7
15	101.06	86.0	93.0	93.9
16	99.5	84.1	91.3	91.5
17	98.19	80.2	89.9	90.6
18	95.67	77.8	87.2	88.7
19	93.8	73.8	83.3	85.8
20	92.3	—	79.4	82.8
21	90.31	—	74.3	79.1
23	88.3	—	—	73.3

Table S5. Raw data of CA on AHS-MIS_y at 25°C. (Fig.4)

a) y=1, 2

Time (min)	AHS-MIS_1				Blank	AHS-MIS_2			
	Blank	0.1M MA	0.01M MA	0.1M EPH		0.1M MA	0.01M MA	0.1M EPH	
0	136.3	130.0	133.2	138.9	138.3	149.8	143.8	145.7	
5	133.9	128.3	131.9	138.6	133.5	147.1	141.5	143.8	
10	132.3	127.0	131.0	137.8	127.3	145.6	137.1	142.8	
15	130.0	125.1	129.5	136.4	121.8	144.8	134.4	142.7	
20	127.3	123.0	127.7	133.5	120.2	144.4	132.5	142.5	
25	125.0	121.4	126.4	132.0	107.6	140.0	122.1	141.1	
30	122.8	119.0	124.5	130.5	100.2	138.6	121.6	140.2	
35	119.0	116.3	122.0	128.6	92.6	135.4	117.1	140.3	
40	114.2	112.9	119.1	126.7	80.4	130.6	109.7	139.9	
45	108.4	108.6	115.8	123.9	69.5	128.6	107.2	138.5	
50	96.8	101.1	109.3	122.4	58.6	120.9	97.2	136.3	
55	82.8	91.6	96.7	119.0	47.3	109.9	86.5	131.6	
60	73.4	82.8	89.7	116.0	41.3	104.7	84.0	133.5	

b) y=3, 4

Time (min)	AHS-MIS_3				Blank	AHS-MIS_4			
	Blank	0.1M MA	0.01M MA	0.1M EPH		0.1M MA	0.01M MA	0.1M EPH	
0	132.0	128.8	126.8	132.3	137.7	138.7	138.0	141.2	
5	126.7	125.7	121.6	128.0	135.9	136.8	136.3	139.2	
10	123.4	124.4	118.5	126.5	133.9	135.0	134.2	137.2	
15	121.4	123.6	117.2	125.7	130.8	132.2	131.4	134.3	
20	119.1	122.0	115.2	124.1	127.5	129.6	128.8	131.2	
25	116.2	119.7	113.3	121.7	130.1	132.8	132.2	134.7	
30	114.0	118.1	111.2	120.0	118.9	122.1	121.5	124.3	
35	109.4	114.8	106.3	116.7	112.6	116.7	116.3	118.4	
40	102.7	110.1	103.9	111.7	104.2	110.5	110.6	112.0	
45	100.2	108.9	102.0	110.5	97.9	104.4	104.4	105.8	
50	92.3	102.0	94.2	103.2	86.9	94.8	95.9	95.6	
55	86.1	96.8	88.7	97.2	76.2	84.6	86.4	85.5	
60	80.6	91.4	86.3	92.1	62.9	72.7	79.2	75.7	

Table S6. Raw data of CA on AHS-MA-0.1 at 25°C after 14days since the surface was made. (Fig.S11)

Time(min)	Blank	0.1M MA	0.01M MA	0.1M EPH
0	134.2±1.4	120.2±4.2	121.9±2.1	133.4±1.8
4	134.3±1.4	112.0±3.3	119.0±3.1	133.1±2.6
8	133.4±0.9	108.6±2.6	117.1±2.7	131.6±1.6
12	133.4±1.6	107.1±2.0	116.9±2.6	131.1±1.6

Supplementary Information

19	133.9±2.0	103.4±4.5	116.3±3.3	131.5±2.5
24	133.6±1.1	99.3±6.9	112.7±5.7	130.5±5.6
28	132.4±1.4	92.9±5.9	111.1±3.2	128.1±4.1
35	131.4±0.9	85.1±8.9	109.9±5.6	127.0±4.7
40	129.4±1.5	73.6±7.4	106.8±6.3	124.2±5.7
44	126.2±1.2	63.0±9.1	102.1±7.7	120.6±5.3
50	123.0±1.0	56.7±10.3	96.7±9.0	116.3±7.0
